

# LWA1 Pointing Error and Correction

LWA Memo #194

Version 2

Jayce Dowell\*      Caleb Grimes†

March 21, 2013

## Contents

<b>1</b>	<b>Introduction</b>	<b>3</b>
<b>2</b>	<b>Data</b>	<b>3</b>
<b>3</b>	<b>Pointing Analysis</b>	<b>3</b>
<b>4</b>	<b>Results</b>	<b>4</b>
<b>A</b>	<b>A Brief History of the LWA1 Pointing Error and Correction</b>	<b>6</b>
<b>B</b>	<b>Conversion of Azimuth/Elevation to and from Topocentric Coordinates</b>	<b>7</b>
<b>C</b>	<b>Document History</b>	<b>7</b>

## List of Tables

1	Right Ascension and Declination Pointing Errors . . . . .	8
---	---	---

## List of Figures

1	On-Sky Source Distribution . . . . .	9
---	--------------------------------------	---

---

\*University of New Mexico. E-mail: [jdowell@unm.edu](mailto:jdowell@unm.edu)

†University of New Mexico. E-mail: [caleb.grimes49@gmail.com](mailto:caleb.grimes49@gmail.com)

2	Example Drift Scan Set . . . . .	10
3	Results of Pointing Correction . . . . .	11

# 1 Introduction

This memo documents the LWA1 pointing error and the correction applied to minimize this error. Although the correction presented in this memo is effective at minimizing the error, the source of the error is still unknown. This memo is structured as follows: Section 2 lists the observations taken in order to determine the pointing error and §3 presents the analysis method. The results of the analysis, including the best-fit correction, are given in §4. Finally, a brief history of the pointing error and corrections for it are provided in Appendix A.

## 2 Data

The data used to determine the pointing correction were collected between March 6th and March 10th, 2013. The data consist of 17 drift scan sets of 3C123, Cas A, Cyg A, Her A, Tau A, and Vir A at elevations greater than 30 degrees. The positions of each of the sources are shown on the sky in Figure 1. Each drift scan set is comprised of three one-hour beam former observations: one centered on the source, one offset from the source by one degree to the south, and one offset from the source by one degree to the north. For all beam former observations, the tunings were set to 38 and 74 MHz with a bandwidth of 4.9 MS/s. It should be noted that only the 74 MHz data was used to determine the pointing error due to the higher angular resolution at this frequency.

After collecting the data, the pointing error for each drift scan set was determined. First, the time when the source transits the beam was determined by fitting a Gaussian to the power associated with the inner 75% of the bandpass as a function of time. This provides the time of transit, the peak power for the beam, and an estimate of the full width at half power for the beam. The observed beam transit time was then differenced from the expected beam transit time for the source to determine the right ascension error. The observation within each set with the highest peak power was adopted as the best measurement of this error. The declination error was determined in a similar fashion, i.e., by fitting a Gaussian to the peak power measurements as a function of declination offset. Since each drift scan set contains only three data points, the full width at half power from the right ascension fits was used to increase the number of free parameters in the fit. An example of the spectrometer data and the above procedure for one Cyg A set is shown in Figure 2. The results of the right ascension and declination error determinations for all sources are listed in Table 1.

## 3 Pointing Analysis

### 3.1 Mathematical Background

Once the right ascension and declination errors were determined for all sources, the errors were fit to find the best pointing correction. The resulting pointing correction is implemented within the monitor and control software (MCS) as a rotation about an axis with three parameters:  $\theta$ ,  $\phi$ , and  $\psi$ .  $\theta$  and  $\phi$  define the orientation of the rotation axis with  $\theta$  and  $\phi$  related back to azimuth and elevation via:

$$\begin{aligned} \text{azimuth} &= 90^\circ - \theta; \\ \text{elevation} &= 90^\circ - \phi. \end{aligned} \tag{1}$$

The final parameter,  $\psi$ , defines the amount of rotation about this axis following the right hand rule. The rotation matrix<sup>1</sup>,  $\mathbb{R}$ , is defined as:

$$\mathbb{R} = \mathbb{I} \cos \psi + [\vec{u}]_x \sin \psi + (\vec{u} \otimes \vec{u})(1 - \cos \psi), \quad (2)$$

where  $\mathbb{I}$  is the identity matrix,  $\vec{u}$  is the rotation axis defined as:

$$\vec{u} = \begin{bmatrix} u_x \\ u_y \\ u_z \end{bmatrix} = \begin{bmatrix} \cos \phi \sin \theta \\ \sin \phi \cos \theta \\ \cos \theta \end{bmatrix}, \quad (3)$$

$[\vec{u}]_x$  is the cross-product matrix of  $\vec{u}$ , and  $\vec{u} \otimes \vec{u}$  is the tensor product of  $\vec{u}$  with itself. The rotation matrix is applied to the topocentric coordinates for the specified pointing,  $\vec{c}$ , to yield the topocentric coordinate of the corrected pointing,  $\vec{b}$ , through:

$$\vec{b} = \mathbb{R}\vec{c}. \quad (4)$$

See Appendix B for a discussion about how to convert azimuth/elevation coordinates to and from topocentric coordinates.

### 3.2 Fitting

The fitting routine employed a brute-force approach to find the best-fit rotation axis. Possible rotation axes were searched in two degree increments for  $\theta$  and  $\phi$  and in one degree increments for  $\psi$ . The parameter minimized during the fitting was the square root of the mean squared (RMS) error. After the minimum RMS error was found with the coarse search, a finer search was performed around the best-fit rotation axis. This finer search examined a range of  $\pm 8$  degrees in  $\theta$  and  $\phi$ , and  $\pm 4$  degrees in  $\psi$  around the coarse search solution at a resolution of one degree in  $\theta$  and  $\phi$  and 0.5 degrees in  $\psi$ . A final search was then performed on all three parameters with a range of  $\pm 4$  degrees in  $\theta$  and  $\phi$ , and  $\pm 2$  degrees in  $\psi$  around the coarse search solution at a resolution of 0.1 degrees for all parameters.

## 4 Results

Using the pointing errors listed in Table 1 and the procedure outlined in §3, the best-fit rotation axis was determined to be:

$$\begin{aligned} \theta &= 28.9^\circ; \\ \phi &= 127.6^\circ; \\ \psi &= 0.6^\circ. \end{aligned}$$

This corresponds to an axis approximately 61 degrees above the northwest horizon (azimuth of  $\sim 323$  degrees). Figure 3 compares the total pointing error from Table 1 with the results of applying the above correction. Before the correction, the mean pointing error was 0.39 degrees. After correction, the mean pointing error was reduced to 0.10 degrees. The post-correction pointing errors also do not

<sup>1</sup>For more information about the rotation matrix, see [http://en.wikipedia.org/wiki/Rotation\\_matrix](http://en.wikipedia.org/wiki/Rotation_matrix) and references therein.

show a strong correlation with elevation, indicating that the best-fit rotation should be applicable to a wide range of elevations. For reference, the best-fit line to the residual pointing error as a function of elevation has a slope of about 0.002 degrees of error per degree of elevation.

## A A Brief History of the LWA1 Pointing Error and Correction

**March 19, 2012** First indications of a pointing error reported in beam former data by Steve Ellingson.

**Late March to early April, 2012** RA and dec. corrections manually applied to SDFs by the LWA1 operators.

**April 4, 2012** LWA1 operators begin using the `shiftSDF.py` utility to apply a RA and dec. correction to SDFs before running. The correction is -7 minutes in RA and +1 degree in declination.

**April 10, 2012** Jake Hartman measures the pointing error in the PASI images and quantifies the error as a rotation about an axis.

**July 12, 2012** Patch applied to MCS to automatically apply a pointing correction based on a rotation about an axis. The initial correction applied is based off the PASI images.

**July 17, 2012** The PASI-based correction appears to overshoot the declination correction by 1 degree and undershoot the RA correction by 4 minutes based on a transit observation of Cyg A.

**August 7, 2012** Re-calibration of the delays based on observations of the Sun during a solar burst applied to the SSMIF.

**August 9, 2012** New pointing correction applied to the SSMIF based on a single fit to the transit of Cyg A.

**August 20, 2012** Campaign started to observe Cas A, Cyg A, Tau A, and Vir A to better determine the pointing correction.

**August 29, 2012** New pointing correction based on the new data found and applied to the SSMIF.

**September 1, 2012** Observations at transit for Cyg A, Cas A, and Tau A show the new correction to be working at least for transiting sources at low zenith angles near the meridian.

**September 14, 2012** A more systematic campaign started to observe Cas A, Cyg A, Tau A, and Vir A to better determine the pointing correction. This campaign will address the sky coverage limitations of the previous campaign.

**September 24, 2012** New pointing correction determined and applied to the SSMIF. A long track of Cyg A was started to verify the pointing correction. The long track indicated poor pointing away from transit.

**September 26, 2012** The MCS pointing correction calculation appears to have two typographical errors leading to the correction applied to SDFs to be in error (see Figure 4 in version 1 of this memo). These were corrected and a new long track of Cyg A was obtained. The new track showed the pointing correction to be working.

**March 6, 2013** An error was found in the cable model used for the previous calibrations. This was corrected and a new calibration was derived from TBW self-calibration methods. The overall pointing error was smaller with the new calibration.

**March 10, 2013** Finished a second round of pointing checks and determined the new best-fit rotation.

## B Conversion of Azimuth/Elevation to and from Topocentric Coordinates

In order for the rotation matrix listed in Equation 2 to be applied, azimuth and elevation coordinates for the pointing need to be converted to topocentric coordinates. The topocentric coordinates are defined with the positive x-axis pointing east and the positive z-axis pointing toward zenith. For a given azimuth,  $az$ , and elevation,  $el$ , the corresponding topocentric coordinates,  $\vec{c}$ , are given by:

$$\vec{c} = \begin{bmatrix} c_x \\ c_y \\ c_z \end{bmatrix} = \begin{bmatrix} \cos(90^\circ - az) \sin(90^\circ - el) \\ \sin(90^\circ - az) \cos(90^\circ - el) \\ \cos(90^\circ - az) \end{bmatrix}. \quad (5)$$

After the rotation matrix has been applied according to Equation 4, the resulting topocentric coordinates can be converted back to azimuth and elevation values using:

$$\begin{aligned} az &= 90^\circ - \arctan\left(\frac{c_y}{c_x}\right); \\ el &= 90^\circ - \arccos c_z. \end{aligned} \quad (6)$$

## C Document History

- Version 2 (March 21, 2013)
  - Revised text for clarity.
  - Updated for the latest SSMIF (`SSMIF_130310.txt`).
- Version 1 (October 2, 2012)
  - Initial version.

Source Name	UTC Observation Midpoint [YYYY/MM/DD HH:MM:SS]	Azimuth [DDD:MM.SS.S]	Elevation [DD:MM.SS.S]	RA Error [HH:MM:SS.SS]	Dec. Error [DD:MM:SS.S]
3C123	2013/03/06 00:52:43	179:59:11.4	85:37:34.3	0:00:32.02	0:03:51.1
TauA	2013/03/06 01:49:59	179:59:32.1	77:57:03.7	0:01:15.03	0:08:14.8
CygA	2013/03/06 16:12:12	0:00:08.5	83:18:05.1	0:00:48.08	0:12:07.6
VirA	2013/03/07 05:22:50	103:23:08.0	40:00:31.9	0:02:38.71	0:19:23.4
VirA	2013/03/07 07:10:27	131:00:29.5	59:59:30.9	0:01:36.98	0:16:59.8
VirA	2013/03/07 08:41:06	180:00:07.9	68:14:40.1	0:01:35.65	0:13:14.1
TauA	2013/03/08 02:54:31	237:38:44.4	70:00:48.4	0:01:13.60	0:07:35.4
TauA	2013/03/08 04:36:01	264:08:41.0	50:01:00.2	0:01:29.07	-0:02:53.7
CygA	2013/03/08 12:43:26	65:08:15.1	49:59:50.2	0:02:28.37	0:23:03.6
HerA	2013/03/09 10:54:38	130:00:49.4	49:59:15.1	0:01:57.17	0:13:06.6
HerA	2013/03/09 12:52:48	179:59:56.7	60:53:57.3	0:01:36.36	0:06:28.0
CasA	2013/03/09 14:54:21	38:34:56.0	40:00:01.3	0:02:22.21	0:24:52.0
CasA	2013/03/09 17:42:20	26:23:56.7	60:00:02.2	-0:00:04.58	0:19:42.5
CasA	2013/03/09 19:23:59	359:59:51.4	65:11:05.1	-0:00:38.77	0:13:00.2
CygA	2013/03/09 21:10:08	301:19:03.7	30:00:15.9	0:02:20.83	-0:03:43.9
CasA	2013/03/09 22:35:28	323:18:48.6	49:59:50.3	-0:00:35.60	-0:05:32.6
CasA	2013/03/10 01:12:04	323:24:47.4	30:00:15.7	0:00:05.97	-0:22:46.6

Table 1: List of Drift Scan Sets used to Determine the Pointing Error

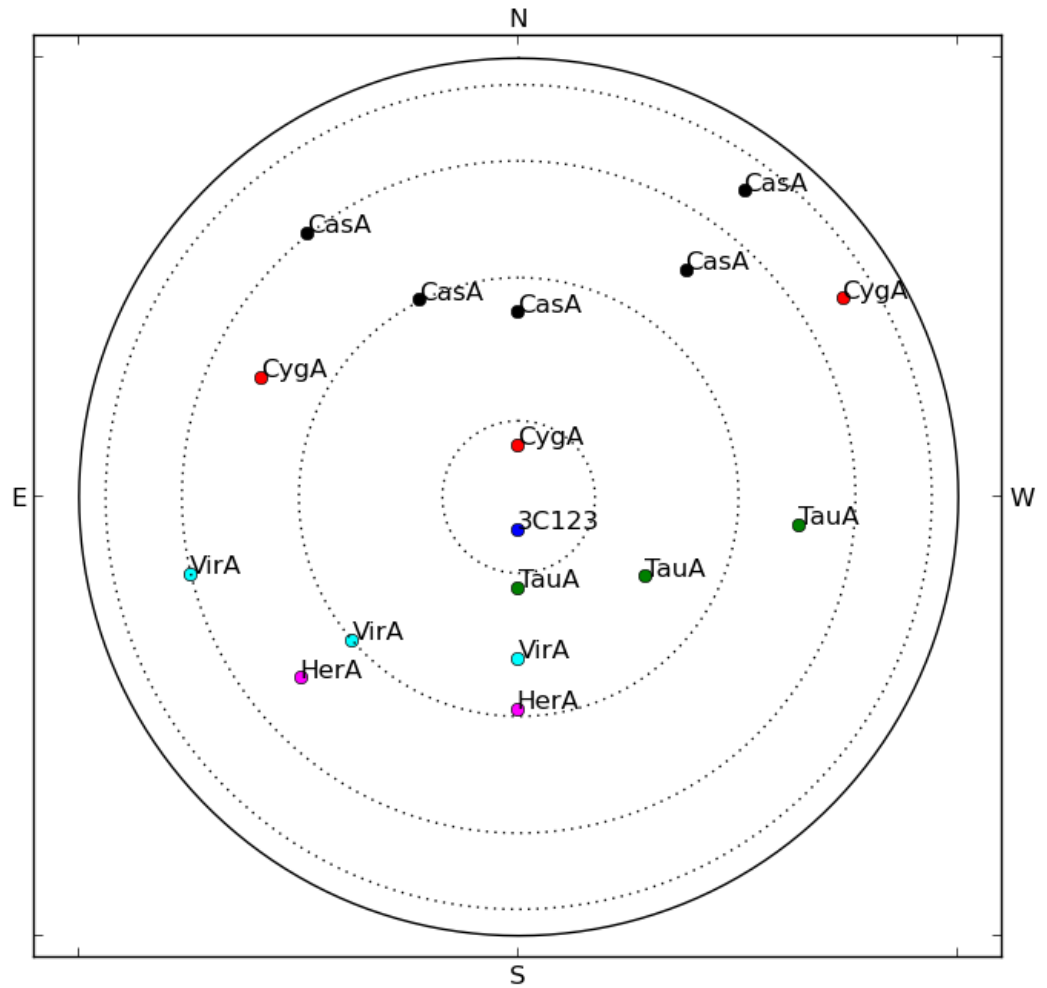


Figure 1: On-sky distribution for the sources listed in Table 1. North is up and east is to the left. Lines of constant elevation are marked by dotted lines at 20°, 40°, 60°, and 80°.

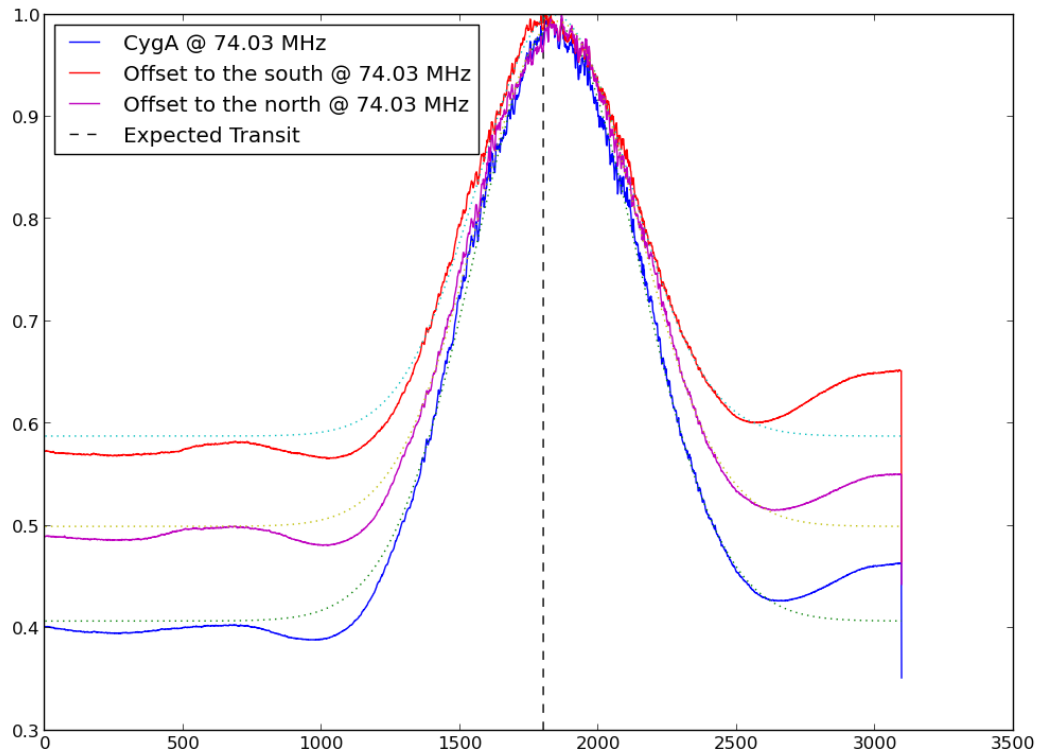


Figure 2: Plot of the spectrometer data collected for the Cyg A run on March 6, 2013. The x-axis is in UTC time while the y-axis is in linear power. The best-fit Gaussians for each of the beams are plotted as dashed lines while the beam transit times determined from the Gaussian fits are plotted as dotted lines. For this data, the error in RA is  $\sim 1$  minute and the error in declination is  $\sim 13'$ .

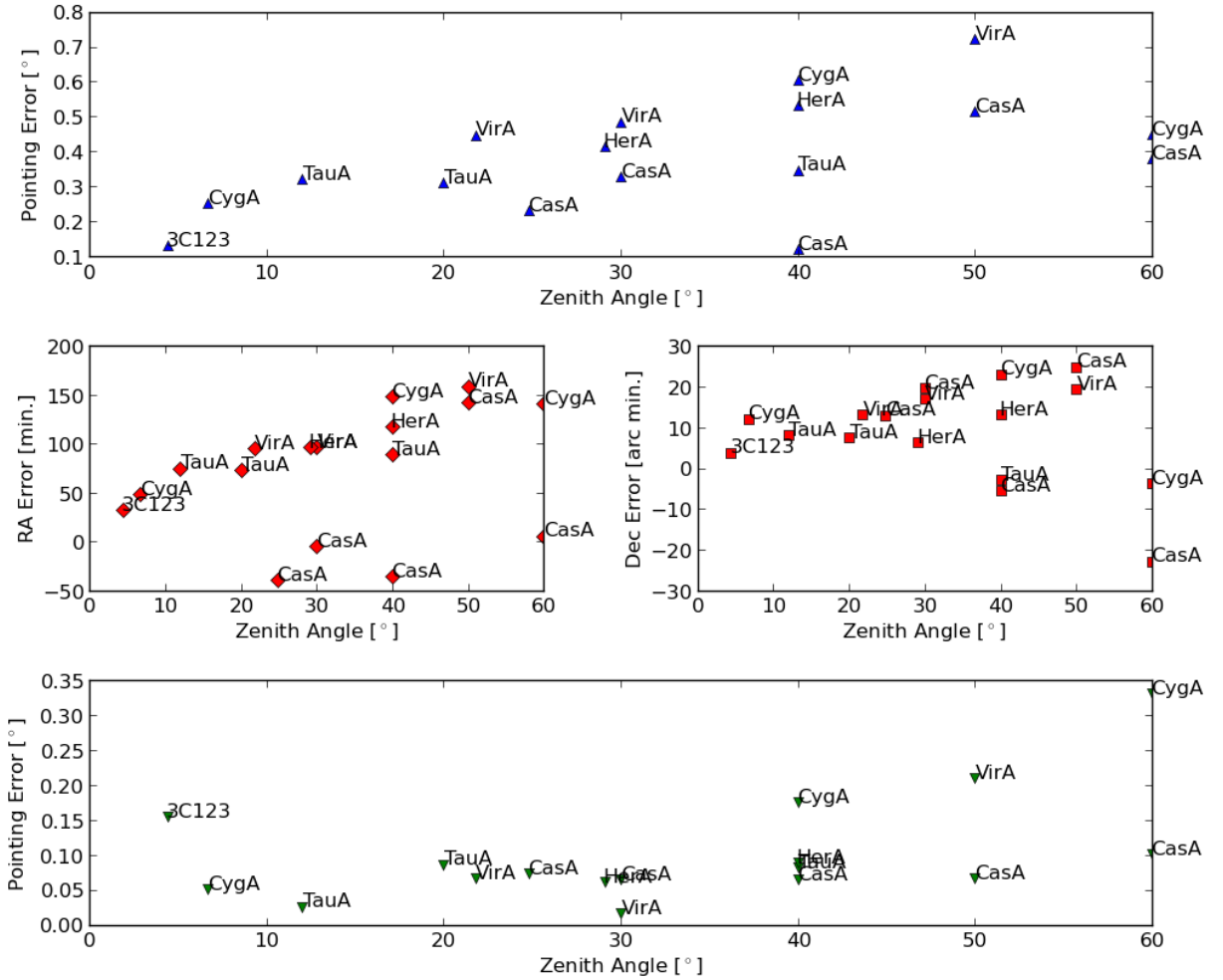


Figure 3: Comparison between the raw pointing offsets (total – top panel; by RA and Dec. – middle two panels) and the corrected pointing offsets (bottom panel). The source associated with each data point is listed to the upper right. Before correction the mean pointing error is  $\sim 0.4^\circ$  and the mean error is  $\sim 0.1^\circ$  after correction.